Article

Current Biology

Visually guided and context-dependent spatial navigation in the translucent fish *Danionella cerebrum*

Highlights

- Adult *Danionella cerebrum* (DC) exhibit strong negative phototaxis
- DC are capable of learning a Morris water maze-like spatial navigation task
- DC use environmental visual cues to solve the spatial navigation task
- Performance in this task is modulated by the visual environmental context

Authors

Timothy J. Lee, Kevin L. Briggman

Correspondence

timothy.lee@mpinb.mpg.de (T.J.L.), kevin.briggman@mpinb.mpg.de (K.L.B.)

In brief

The translucent fish *Danionella cerebrum* (DC) are a promising systems neuroscience animal model. Lee and Briggman show that adult DC exhibit negative phototaxis and apply this as a motivator in a Morris water maze-like spatial navigation task. DC use visual cues to learn this task; their performance is modulated by the environmental visual context.

Lee & Briggman, 2023, Current Biology *33*, 1–11
December 18, 2023
https://doi.org/10.1016/j.cub.2023.11.030

CellPress

Please cite this article in press as: Lee and Briggman, Visually guided and context-dependent spatial navigation in the translucent fish *Danionella cerebrum*, Current Biology (2023), https://doi.org/10.1016/j.cub.2023.11.030

Current Biology

CellPress
OPEN ACCESS

Article

Visually guided and context-dependent spatial navigation in the translucent fish *Danionella cerebrum*

Timothy J. Lee[1,2,*] and Kevin L. Briggman[1,*]
[1]Max Planck Institute for Neurobiology of Behavior - caesar, Department of Computational Neuroethology, Ludwig-Erhard-Allee 2, Bonn, 53175 North Rhine-Westphalia, Germany
[2]Lead contact
*Correspondence: timothy.lee@mpinb.mpg.de (T.J.L.), kevin.briggman@mpinb.mpg.de (K.L.B.)
https://doi.org/10.1016/j.cub.2023.11.030

SUMMARY

Danionella cerebrum (DC) is a promising vertebrate animal model for systems neuroscience due to its small adult brain volume and inherent optical transparency, but the scope of their cognitive abilities remains an area of active research. In this work, we established a behavioral paradigm to study visual spatial navigation in DC and investigate their navigational capabilities and strategies. We initially observed that adult DC exhibit strong negative phototaxis in groups but less so as individuals. Using their dark preference as a motivator, we designed a spatial navigation task inspired by the Morris water maze. Through a series of environmental cue manipulations, we found that DC utilize visual cues to anticipate a reward location and found evidence for landmark-based navigational strategies wherein DC could use both proximal and distal visual cues. When subsets of proximal visual cues were occluded, DC were capable of using distant contextual visual information to solve the task, providing evidence for allocentric spatial navigation. Without proximal visual cues, DC tended to seek out a direct line of sight with at least one distal visual cue while maintaining a positional bias toward the reward location. In total, our behavioral results suggest that DC can be used to study the neural mechanisms underlying spatial navigation with cellular resolution imaging across an adult vertebrate brain.

INTRODUCTION

Spatial navigation—the ability to plan and execute self-directed motion based on sensory cues—is an ethologically relevant behavior observed across a wide variety of phyla.[1] Numerous species, ranging from honeybees to humans, have been studied for their navigational abilities.[2–19] Historically, mammalian animal models (most commonly rodents) have been utilized, in part due to their ability to learn and solve complex spatial navigation behavioral tasks,[5,6,20–22] including the Morris water maze.[23] Simple motivators, such as food or water rewards, are often used to drive goal-oriented navigational behavior.[24] Using these behavioral paradigms, specific brain regions that underlie spatial navigation have been identified in mammals,[25–28] but comparatively little is known about how, at a mechanistic level, these regions work together to generate navigation behaviors. One limitation is the ability to functionally record from and anatomically trace the neuronal circuits underlying these behaviors in relatively large mammalian brains. Hence, our understanding of spatial navigation, and the underlying neuronal mechanisms, remains fragmented.

In parallel, the field of systems neuroscience has seen great strides made in the unbiased whole-brain optical imaging of smaller, awake, behaving animals, such as *Caenorhabditis elegans*,[29,30] *Drosophila melanogaster*,[31–33] and larval *Danio rerio*.[34,35] When combined with volume electron microscopic reconstructions, biologically plausible models of neuronal circuits that support a given behavior can be developed.[36–39] The larval zebrafish, in particular, has been shown to be advantageous for this experimental approach.[39–44] However, compared with mammals, it has been more difficult to train larval zebrafish to associate visual cues with discrete locations in space. This is perhaps due to a delay in the ability of larvae to form associations until later developmental stages.[18,45]

The recent introduction of *Danionella cerebrum* (DC) as a systems neuroscience animal model shows great potential for the mechanistic study of circuits underlying various cognitive processes.[46–50] Similar to larval zebrafish, the transparency and small size of DC make them suited for whole-brain optical imaging at developmental stages many months post-fertilization.[51] However, their visual spatial navigational abilities are currently unknown. Other teleost fish, such as adult zebrafish and goldfish, are capable of solving complex spatial navigation tasks in which learned associations are used to motivate spatial navigation.[11–19] Indeed, teleost fish can employ both egocentric and allocentric navigational strategies,[11–19] mirroring the prowess of mammals. Therefore, we aimed to establish a paradigm for probing spatial navigation in DC and elucidating their navigational abilities.

We identified phototaxis as a motivator for a task inspired by the Morris water maze.[23] Through a series of cue manipulations, we found that DC use visual cues to solve the task. We also

Please cite this article in press as: Lee and Briggman, Visually guided and context-dependent spatial navigation in the translucent fish *Danionella cerebrum*, Current Biology (2023), https://doi.org/10.1016/j.cub.2023.11.030

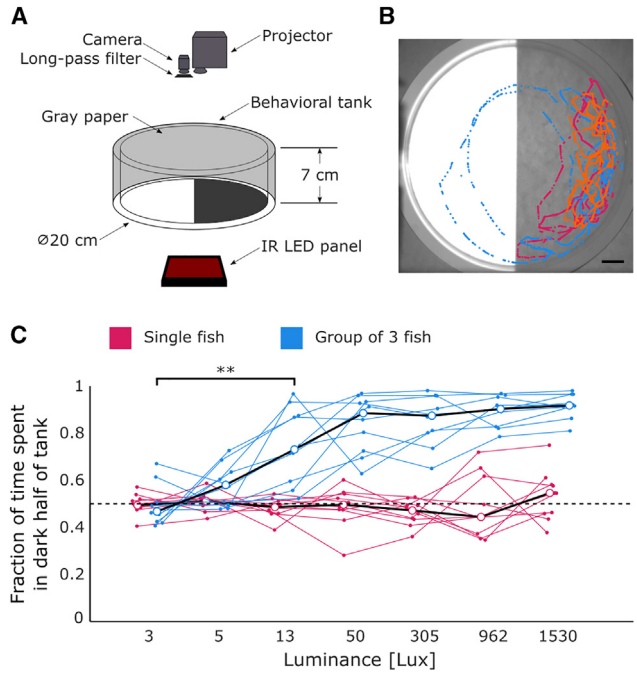

Figure 1. DC exhibit negative phototaxis

(A) Experimental setup for testing phototaxis.

(B) Image of behavioral arena, with the long-pass filter removed and overlaid fish trajectories, depicts the maximal contrast displayed during testing. Scale bars, 20 mm.

(C) Quantification of phototaxis in individuals (magenta) and groups (blue) of DC. Individual fish and groups are linked with lines. White circles represent median values (group condition: n = 10 groups of three DC [30 total fish]; individual condition: n = 10 fish; paired t test; **$p < 0.01$; $p = 0.0016$).

See also Figure S1.

found that DC are capable of context-dependent navigation by manipulating cues that are distal vs. proximal to a reward location. In this work, we defined visual "context" to include unique visual cues that laid distal to and, at times, out of sight from the goal location (as in Zhao et al.[52]). Our results lay a foundation for future work to study the neuronal mechanisms underlying spatial navigation across the adult vertebrate brain of DC.

RESULTS

DC exhibit negative phototaxis

We characterized the phototactic behavior in adult (~3 months old) DC, an age at which we expected robust associative learning, based on previous work in adult teleost fish.[11–19,45] Fish were placed in a circular arena illuminated from above with a digital projector (Figure 1A) and the walls surrounded with gray paper. For each trial, one half of the arena was illuminated with white light of a selected luminance while the other half remained dimly lit (Figure 1B). Because DC are known to be a schooling fish species,[46,48,50] we quantified phototaxis in individuals as well as groups of three conspecific fish. Individual DC did not display a consistent phototactic preference for the dark or light region (Figures 1C and S1A), although we noted an increased variability in phototactic preference among individuals with increasing luminance on the bright half of the arena (Figure S1B). Individual fish were observed to frequently swim in circles around the border of the arena (see representative example in Figure S1A). In contrast, for groups of three fish, we observed an increased dark preference as the luminance was elevated (Figures 1C and S1C). This preference was already observable at low illumination levels (Figure 1C, 3 vs. 13 lux). Group size has been shown to influence vision-based navigation in schooling fish[53]; therefore, the lack of group dynamics in solitary DC could explain their variable phototactic preference. As an additional comparison, groups of 3- to 4-week-old juvenile zebrafish of a similar body size to adult DC exhibited negative phototaxis under the same conditions but to a lesser extent than adult DC (Figure S1D).

DC are capable of learning a Morris water maze-like spatial navigation task

We next explored whether dark preference (or, alternatively, light aversion) could be utilized as a reinforcing stimulus to develop a place preference in a spatial navigation task. For this, and all remaining experiments, fish were tested in groups of three to ensure consistent phototactic behavior. We designed a delayed reward paradigm in a circular arena surrounded by eight unique visual cues on the walls and consisting of four phases (Figure 2A). Within each trial, (1) the arena was uniformly illuminated from above with dim light sufficient for the cues to be visible for 60 s ("DIM"); (2) illumination was increased to an intensity measured to induce negative phototaxis (Figure 1C) for 20 s ("LIGHT"); (3) under the same high intensity illumination, a reward location was revealed by projecting a dark spot in front of one of the visual cues for 45 s ("REWARD"); and (4) the illumination was shuttered for 60 s so that the cues were not visible to the fish ("DARK"). Our goal was to probe whether DC were capable of learning the reward location relative to the visual cues and, if so, reporting this association by anticipating and swimming to the location of the dark spot (the reward location) during the LIGHT phase prior to the spot appearing during the REWARD phase. We quantified performance by measuring the Euclidean distance between the centroids of each fish and the center of the reward location (i.e., "distance-to-target" or "performance") for each video frame (Figures 2B and 2C). The performance of a representative group of fish and associated trajectories (Figure 2C) are plotted for the first trial from the first day of training and the first and thirtieth trial from the third day of training, at which point the fish had learned the association.

During the DIM and DARK phases, fish dispersed throughout the arena (Figure 2C). During the REWARD phase, performance fell below the radius of the reward zone (<4 cm; Figure 2C), reflecting the negative phototaxis we previously measured (Figure 1C). Examination of the LIGHT phase, in which the reward had not yet appeared, revealed an anticipation of the reward location by the thirtieth trial that was not observed in the first trial of the first or third day of training (Figure 2C), suggesting a learned association between the visual cues and the reward location. During the LIGHT phase, performance improved from an initial chance level (6.3 cm) during the course of the first 10–15 trials (30–45 min) and approached the radius of the reward region for the latter trials (Figures 2D and 2E). For groups of fish deemed non-learners, we observed that performance improved very slowly, if at all, during the first 30 trials (Figure 2D). Fish were

Please cite this article in press as: Lee and Briggman, Visually guided and context-dependent spatial navigation in the translucent fish *Danionella cerebrum*, Current Biology (2023), https://doi.org/10.1016/j.cub.2023.11.030

CellPress
OPEN ACCESS

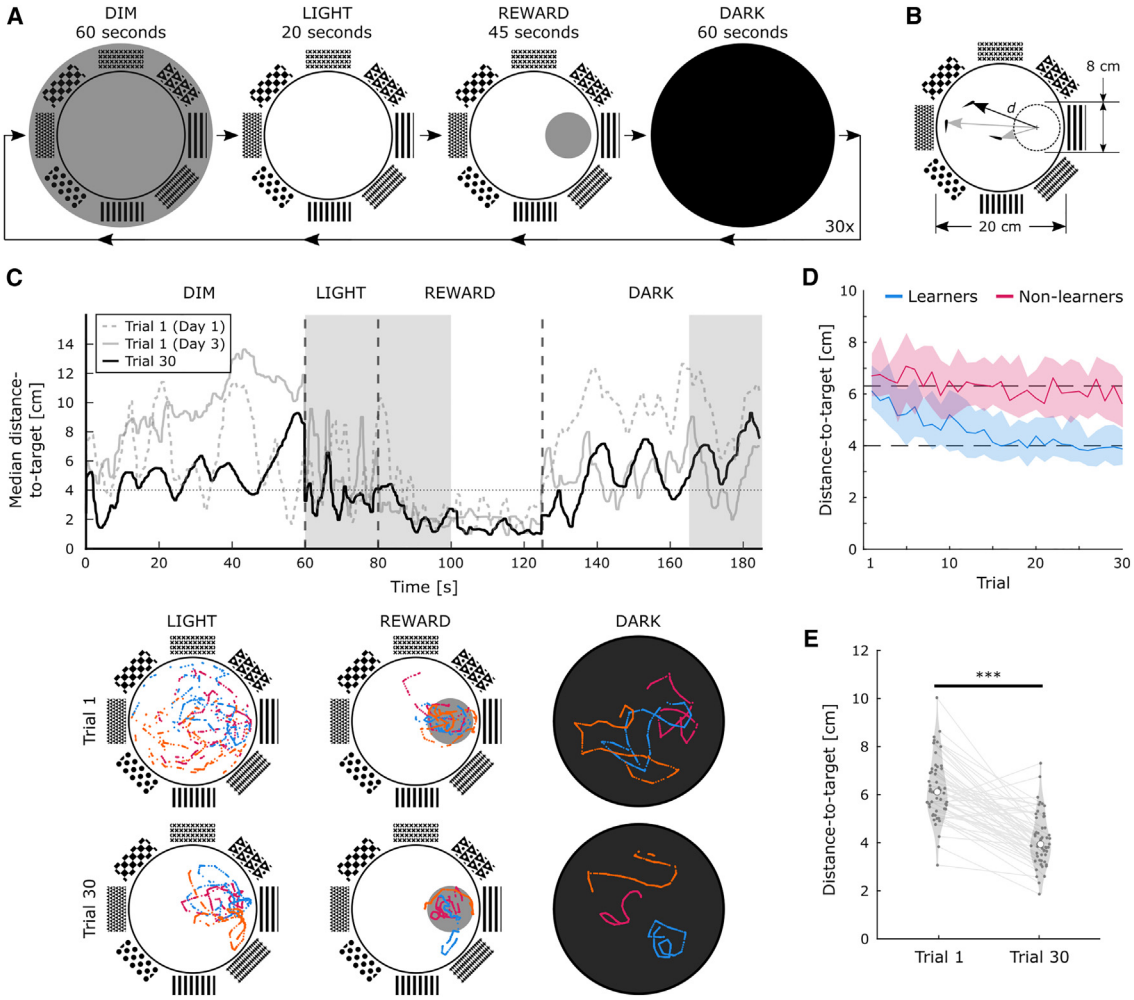

Figure 2. DC are capable of learning a Morris water maze-like spatial navigation task

(A) Diagram of trial structure with four phases.

(B) For each video frame, the Euclidean distance between the centroid of each fish and the center of the reward region (i.e., "target") is measured (black vector, with label *d*).

(C) Example of median distance-to-target for one group of three fish from trial 1 from the first day of training (gray, dashed line), trial 1 from the third day of training (gray solid line), and trial 30 from the third day of training (black). For this group of fish, the learning criterion was met on the third day of training. Vertical dashed lines delineate the trial phases. The horizontal dotted line at 4 cm represents the radius of the reward area. Shaded regions illustrate the 20-s time bins used to compare performance between the trial phases and across trials. Corresponding fish trajectories from day 3 are shown below, with each color representing a unique fish.

(D) Distance-to-target during the LIGHT phase vs. trial number for learner (blue; n = 53 groups) vs. non-learner (magenta; n = 24 groups) groups of fish. Solid lines represent median performance across groups of fish, with shading representing the interquartile range. The horizontal lines represent the reward radius (4 cm) and chance performance (6.3 cm).

(E) The performance distribution of learner groups from trials 1 and 30 (individual points each represent a group of fish; white circles represent median; n = 53 groups of three fish; paired t test, ***$p < 0.001$, $p = 4.2e{-}14$).

See also Figure S2 and Data S1.

able to anticipate the reward location, regardless of the specific cue that lay directly in front of the reward location and so, for consistency, we arbitrarily used horizontal stripes in front of the reward for most groups (Figure S2A).

Given that learning occurs in a group of three fish, it is possible that a preference for shoaling behavior could influence learning (or non-learning) in our task. Therefore, we quantified the sum of inter-fish distances as a metric for each group's cohesiveness (i.e., shoal cohesion). For learning groups, shoal cohesion decreased slightly as performance improved across trials 1–30, consistent with fish learning to confine their swimming pattern near the reward location (Figure S2B). For non-learning groups, shoal cohesion remained relatively constant across trials 1–30. We observed a statistically significant linear correlation between average shoal cohesion and performance for learner groups (Figure S2C, blue), but not for non-learner groups (Figure S2C, orange). Average shoal cohesion was not significantly different between learner and non-learner groups (Figure S2C).

Please cite this article in press as: Lee and Briggman, Visually guided and context-dependent spatial navigation in the translucent fish *Danionella cerebrum*, Current Biology (2023), https://doi.org/10.1016/j.cub.2023.11.030

In total, groups of various cohesiveness were able to learn the task. However, this metric does not reveal intra-group learning dynamics in which a subset of the fish could learn the task and/or drive performance within the task (e.g., a "follow-the-leader" scenario).

Altogether, we concluded that adult DC were capable of learning the reward location, but it remained unclear to what degree visual cues in their environment were used.

DC perform visually guided spatial navigation

Using a series of cue manipulation experiments, we next investigated which visual cues played a role during navigation. An 80-trial session was designed in which eight unique cues were presented for thirty trials, a cue manipulation was performed for twenty trials, and then the original cues were restored for the final thirty trials. The structure within each 3-min trial remained as in Figure 2A. Cue manipulations included cue removal (Figure 3A), cue rotation (Figure 3B), or cue shuffling (Figure 3C). We quantified performance by averaging the distance of each fish to the reward within 20-s time bins: the last 20 s of the DIM phase, the entire 20 s duration of the LIGHT phase, the first 20 s of the REWARD phase, and the last 20 s of the DARK phase. For cue removal sessions, performance during the LIGHT phase improved to near 4 cm within the first 30 trials (Figure 3A, right, LIGHT), indicating a learned association between the visual cues and the reward location. Upon replacement of the cues with a uniform gray background, performance returned to chance levels (6.3 cm), leading to a statistically significant difference in the ability to anticipate the reward location with and without visual cues (Figure 3D, cue removal). Upon restoration of the cues, the performance rapidly returned to near 4 cm. During the DARK phase, the performance remained predominantly near chance, indicating that the fish did not have an innate place preference for a specific region of the arena (Figure 3A, right, DARK). Interestingly, while fish were still able to navigate to within the reward boundary during the REWARD phase, their performance worsened when cues were removed (Figure 3E, cue removal), perhaps indicating that the cues were helpful for the fish to locate the visible reward region. Additionally, to control for the possibility that the physical cue manipulation itself was responsible for this change in behavior, a sham cue removal experiment was conducted and we did not observe a significant change in performance during the LIGHT or REWARD phases (Figures 3A, 3D, and 3E, "sham cue removal"). Altogether, the cue removal experiments indicated that learned visual cues were necessary to anticipate and navigate to the reward location. Additionally, we concluded that the fish were not using any other cues in their environment or external to the arena to anticipate the reward location.

We next examined the strength of the association between the absolute location of the reward relative to the cues by performing a set of cue rotation experiments. We either rotated the reward location and cues together by 90°, 180°, or 270° ("coupled cue rotation") or rotated only the reward location but not the cues ("uncoupled cue rotation") (Figure 3B). During coupled cue rotation, performance remained constant for most groups (Figure 3D, coupled cue rotation), further confirming that fish utilized an association with the visual cues and not potential external cues. However, during an uncoupled rotation of the cues in which the relative location between the reward location and the cues was changed, performance during the LIGHT phase degraded, indicating that fish were initially not able to predict the new location of the reward (Figures 3B, right, LIGHT and 3D, uncoupled cue rotation) but rather continued to prefer the former reward location (Figures S3A and S3B). Throughout the twenty trials of uncoupled cue rotation, performance during the LIGHT phase gradually improved, indicating that the fish were perhaps slowly forming an association between the new location of the reward relative to the cues. Upon reestablishment of the original reward location, fish rapidly returned to their previous performance prior to the uncoupled rotation. During the REWARD phase of the uncoupled cue rotation, negative phototaxis to the reward location was perturbed, as shown by the large distance-to-target values during trials 31–50 (Figures 3B, right, REWARD and 3E, uncoupled, first 20 s); we therefore compared the performance of the first 20 s of the REWARD phase to the last 20 s (Figures 3B, right, REWARD, magenta vs. green and 3E) and found that the perturbation was transient and fish were eventually able to swim to the reward location by the end of the REWARD phase.

Taken together, the cue removal and cue rotation experiments indicated that DC perform visually guided navigation. However, because the reward was always located in front of one of the eight unique visual cues, it remained unclear whether they used one specific cue to navigate (the cue most proximal to the reward) or whether they took advantage of the context of the entire visual environment (including the more distal cues from the reward) to navigate, as has been investigated in other species.[52,54,55] We designed a cue shuffling experiment in which all cues, except for the single cue directly in front of the reward location, were randomly shuffled to a new position (Figure 3C) and hypothesized that, if fish primarily used one proximal cue as a visual landmark, then their ability to solve the task should remain unchanged when the seven other cues were shuffled. During the LIGHT phase, the median performance remained unperturbed following cue shuffling (Figures 3C, right, orange and 3D, "cue shuffle"), similar to that of control fish (Figures 3C, right, gray and 3D, "sham"), indicating that a single cue is sufficient for fish to anticipate the reward location, even when all other cues in the environment are shuffled. This is in agreement with a navigational strategy reported in a variety of species in which a stable landmark in the environment is sufficient to solve a navigation task.[3,56] However, when analyzing the performance of individual groups, we observed that some groups were greatly perturbed by the cue shuffling (Figures 3D, cue shuffle and S3C). Groups were clustered into those that were (3/9) and were not (6/9) perturbed by the cue shuffling (Figures S3D and S3E). We therefore hypothesized that, at least for some groups of fish, distally located unique visual cues played a role in their ability to predict the reward location.

When the last 20 s of the DIM phase was analyzed across all cue manipulations, we observed similar trends as in the LIGHT phase, indicating that many fish were motivated to anticipate the reward location during the DIM phase prior to the onset of the LIGHT phase (Figure S4).

Context-dependent spatial navigation in DC

To investigate the importance of distal contextual spatial information, we designed an experiment in which unique proximal

Please cite this article in press as: Lee and Briggman, Visually guided and context-dependent spatial navigation in the translucent fish *Danionella cerebrum*, Current Biology (2023), https://doi.org/10.1016/j.cub.2023.11.030

CellPress
OPEN ACCESS

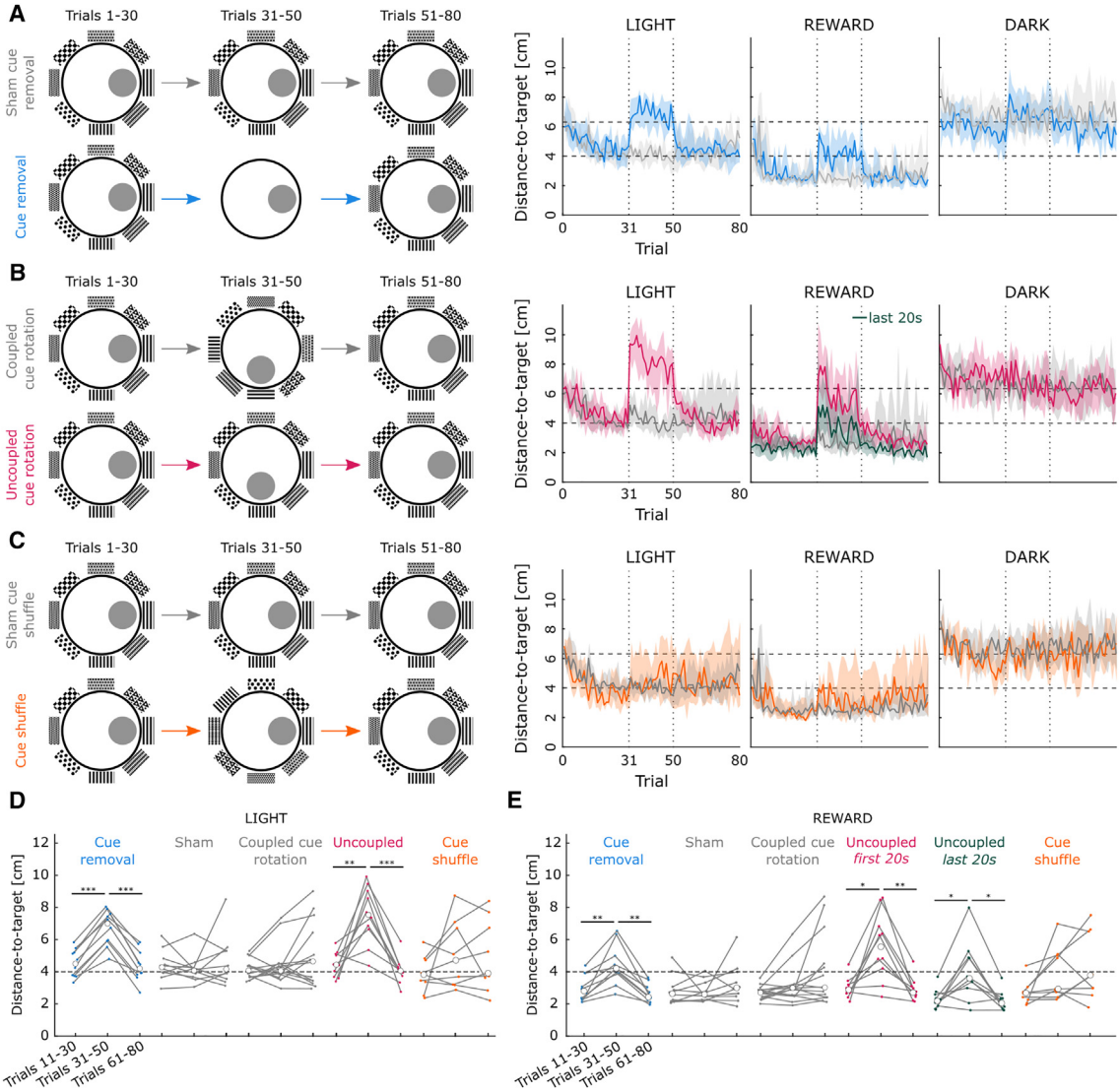

Figure 3. DC perform visually guided spatial navigation

(A) Cue removal experiment, including the cue removal (blue) and sham control (gray) groups. The performance across all trials for each trial phase is shown on the right (cue removal, n = 10 groups; sham cue removal, n = 10 groups).

(B) Cue rotation experiment depicting the uncoupled (magenta; n = 10 groups) and coupled (gray; n = 14 groups) cue rotations.

(C) Cue shuffle experiment depicts the cue shuffled (orange; n = 9 groups) and sham control (gray) group cue manipulation. The sham cue shuffle and sham cue removal from (A) are the same dataset, shown twice for convenience. In (A)–(C), thick lines represent median performance across groups; shading represents interquartile range.

(D) Comparison of performance distributions for the LIGHT phase across trial bins: before the cue manipulation (trials 11–30), during the cue manipulations (trials 31–50), and following the cue manipulation (trials 61–80).

(E) Comparison of performance distributions for the REWARD phase across the same trial bins as in (D).

(D) and (E) Connected points show the change in group performance across trial bins. Open circles represent median performance across groups. Paired t test with Bonferroni correction was used for testing significance; *p < 0.05/m; **p < 0.01/m; ***p < 0.001/m, m = 3; (D, left to right, p = 5.4e−7, p = 4.0e−6, p = 0.0014, p = 9.5e−5; E, left to right, p = 0.0012, p = 3.6e−4, p = 0.0036, p = 0.0011, p = 0.0099, p = 0.0050).

See also Figures S3 and S4 and Data S1.

cues were removed, leaving only the more distal unique cues available as potential landmarks for navigation. These proximal cue removal experiments consisted of 90 trials (Figure 4A) in which the eight unique visual cues were presented for thirty trials. After trial 30, between five and eight unique visual cues most proximal to the reward region were removed and replaced with uniform vertical stripes. With this new subset of unique visual cues, we performed a 120° coupled cue rotation after trial 50 and, after trial 70, the cues were rotated back. Additionally, we placed a circular visual blockade in the center of the tank (Figure 4A) to occlude visual cues that were diametrically opposed to the position of each fish, thereby creating a ring-shaped

Please cite this article in press as: Lee and Briggman, Visually guided and context-dependent spatial navigation in the translucent fish *Danionella cerebrum*, Current Biology (2023), https://doi.org/10.1016/j.cub.2023.11.030

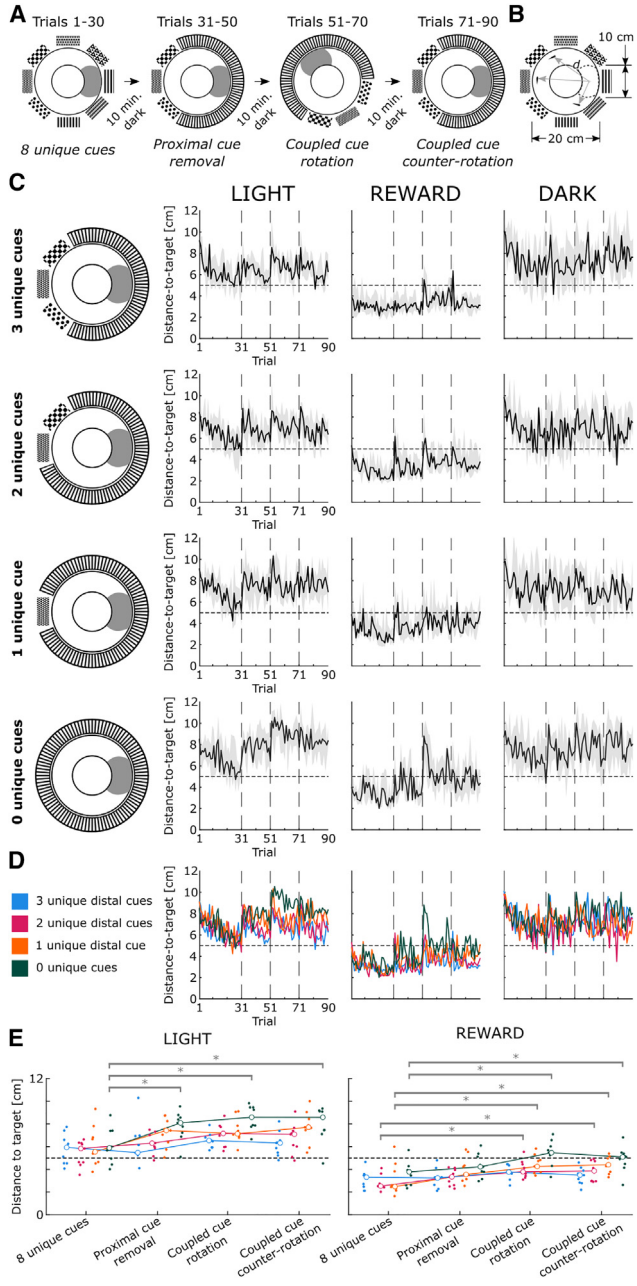

Figure 4. Context-dependent spatial navigation in DC

(A) Diagram depicting the proximal cue removal experiment. A visual blockade (ø10 cm) occluded the view of unique visual cues on the opposite side of the ring-shaped arena. On any given test day, a group of fish were tested for 30 trials with 8 unique visual cues, followed by a proximal cue removal (20 trials), then a coupled cue rotation (20 trials), and finally a coupled cue counter-rotation (20 trials), for a total experiment composed of 90 trials. A 10-min pause in darkness followed each cue manipulation.

(B) For each video frame, the Euclidean distance as in Figure 2B was measured.

(C) A diagram (left) depicts the configuration of the remaining unique visual cues relative to the reward location. The performance of the fish during the LIGHT, REWARD, and DARK phases vs. trial number is shown. (n = 9 groups of three fish; solid black lines represent median performance across groups; gray shading represents interquartile range).

(D) Overlay of median performance, color-coded by number of remaining unique visual cues.

(E) Comparison of group performance across experiment trial bins ("8 unique cues," trials 21–30; "proximal cue removal," trials 41–50; "coupled cue rotation," trials 61–70; and "coupled cue counter-rotation," trials 81–90) and across cue manipulations during the LIGHT and REWARD phases. (Each solid point represents a group; the color depicts the cue manipulation. Open circles represent median performance, connected across trial bins. Dashed line represents diameter of reward area [5 cm]. Paired t test with Bonferroni correction; *$p < 0.05/m$; m = 6 comparisons within each proximal cue removal condition; [E, LIGHT bottom to top: p = 0.00066, p = 0.0063, p = 0.0077; REWARD, bottom to top: p = 0.0082, p = 0.0033, p = 0.0045, p = 0.0042; p = 0.0022, p = 0.0017]).

See also Figure S5 and Data S1.

arena. A 10-min DARK phase was inserted between cue manipulations to allow more time for fish to disperse from the reward region and discourage a strategy of simply not moving in the annular arena to solve the task. We used a similar trial structure as in Figure 2A and performance quantification (Figure 4B), but increased the duration of the DARK phase, again, to allow more time for fish to disperse from the reward region. The performance of fish during the LIGHT phase approached 5 cm (the radius of the reward zone in the annular arena) in the first 30 trials (Figure 4C, LIGHT), across all cue manipulations, demonstrating that DC accurately predicted the reward location in the annular arena with 8 unique visual cues. At trial 31, upon replacement of the five unique cues located proximal to the reward location with a uniform pattern and following the cue rotations (trials 51 and 71) the performance of the fish was transiently perturbed but then gradually improved with subsequent trials, indicating the ability to predict the reward location without proximally located visual cues (Figure 4C, top row, LIGHT). Performance predominantly remained below 5 cm during the REWARD phase, reflecting the fish's negative phototaxis, with transient perturbations following some cue manipulations (Figure 4C, REWARD). As the number of unique visual cues was further reduced from three to zero, we observed a degradation in performance during the LIGHT phase and measured a statistically significant difference when zero unique cues remained compared with the initial trials when all eight cues were present (Figures 4D and 4E, LIGHT). Similar to the cue removal experiments (Figure 3A), the ability of DC to navigate to the reward region during the REWARD phase was perturbed in the absence of unique visual cues (Figures 4D and 4E, REWARD). When binned across trials, we observed a statistically significant degradation in performance during the LIGHT phase as unique visual cues were removed (Figure 5A). In total, these results showed that DC were capable of utilizing distally located visual cues during the LIGHT phase to anticipate the reward location.

A major difference compared with the open arena performance (Figures 2 and 3) was the behavior of DC during the DARK phase in the annular arena (Figure 4C). Although we expected fish to disperse during the DARK phase, they never reached the calculated chance performance in the annular arena (10.2 cm) (Figure 5B). More puzzling was the apparent improvement in performance during the first thirty trials, which should be impossible in the dark (Figure 4C) and indicated that, despite a lengthened DARK phase, the fish were not dispersing following each REWARD phase. When we compared the performance between the corresponding LIGHT and DARK phases for each proximal cue manipulation experiment, we did not find any

Please cite this article in press as: Lee and Briggman, Visually guided and context-dependent spatial navigation in the translucent fish *Danionella cerebrum*, Current Biology (2023), https://doi.org/10.1016/j.cub.2023.11.030

CellPress
OPEN ACCESS

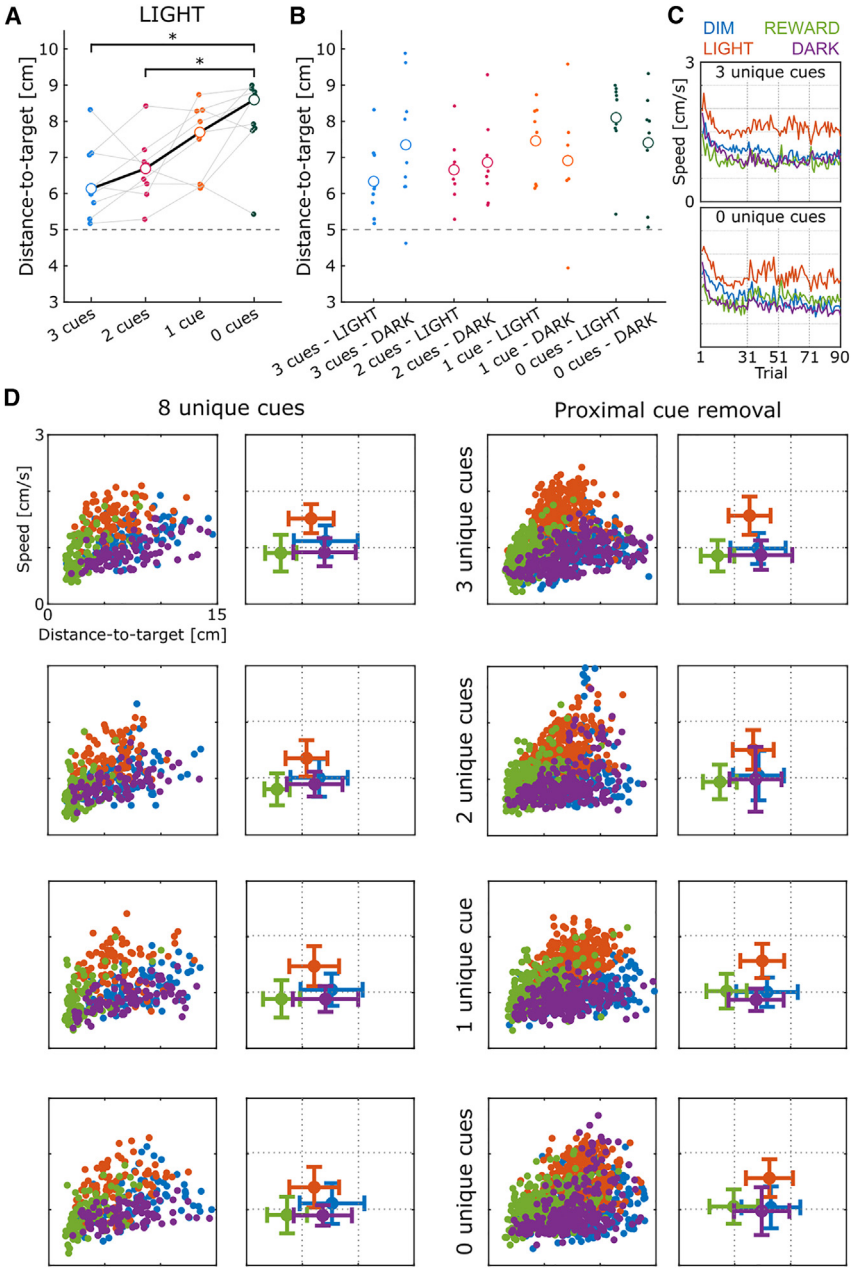

Figure 5. Behavior in proximal cue removal experiments is modulated by luminance

(A) Performance between proximal cue removal experiments during the LIGHT phase, averaged across trials 41–50, 61–70, and 81–90 for each group. Individual solid points and thin gray lines represent individual groups; open circles and thick black lines represent median across groups. Paired t test with Bonferroni correction; *p < 0.05/m, m = 6; top to bottom, p = 0.0037, p = 0.0029 (n = 9 groups).

(B) Pairwise comparisons of performance between the LIGHT and DARK phase for each proximal cue removal experiment condition. Performance was averaged across trials 41–50, 61–70, and 81–90 for each group. Individual points represent individual groups. Paired t test with Bonferroni correction, m = 4. No statistically significant differences were observed.

(C) The average speed for each trial was measured against trial number for the "3 unique cues" (top) and "0 unique cues" (bottom) cue manipulations, color-coded by trial phases. Lines represent the median across groups of fish (n = 9 groups).

(D) Scatter plots showing average speed vs. performance from 8 unique cues trial bin (trials 21–30), and proximal cue removal trial bin (trial 41–50, 61–70, and 81–90) pooling all groups and across the four experiment phases. Color coding same as in (C). The mean and standard deviation for each experiment phase is shown to the right of each scatter plot. Individual data points represent single trials for each group of fish. See also Figure S5.

significant differences in any of the cue conditions (Figure 5B). Accordingly, it was possible the fish had adopted a "stay-in-place" strategy that persisted from the REWARD into the DARK and LIGHT phase. We therefore measured the average speed of the groups as a function of trial number to investigate whether changes in locomotion revealed differences in behavior between the LIGHT and DARK phase that were not revealed by the distance-to-target metric. We observed a reduction in swimming speed during the initial thirty trials (Figures 5C and S5B), perhaps indicating a form of motor adaptation as fish become accustomed to the experiment. The decrease in swimming speed is consistent with DC not fully dispersing in the arena following each REWARD phase (Figure 4C), despite a prolonged DARK phase.

Strikingly, while swimming speeds were similar during the DIM, REWARD, and DARK phases, they were approximately 50% higher during the LIGHT phase (Figures 5C and S5B), indicating a dependency of motor behavior on the ambient illumination.[57] By plotting swimming speed vs. performance for the different proximal cue removal experiments, we observed a trend in which the performance of the fish during the LIGHT phase degraded as unique visual cues were removed (Figure 5D, orange) and less so in the DARK phase (Figure 5D, purple).

Based on the behavioral differences observed during the LIGHT phase, we investigated where in the annular arena DC spent most of their time relative to the visibility of the unique cues. The reduction in the ability of DC to anticipate the reward location as the number of unique cues is reduced is visible in heatmaps of their positions during the LIGHT phase (Figures 6A and S6). Difference heatmaps, calculated by subtracting the locations when proximal cues are removed from when all eight cues are present, illustrate the relative positions DC occupy for each cue manipulation (Figure 6B). Overall, as proximal cues are removed, DC spend proportionally less time near the reward location, where there is often no direct line of sight to the unique visual cues, and more time swimming in regions in which at least one unique visual cue is within sight,

Please cite this article in press as: Lee and Briggman, Visually guided and context-dependent spatial navigation in the translucent fish *Danionella cerebrum*, Current Biology (2023), https://doi.org/10.1016/j.cub.2023.11.030

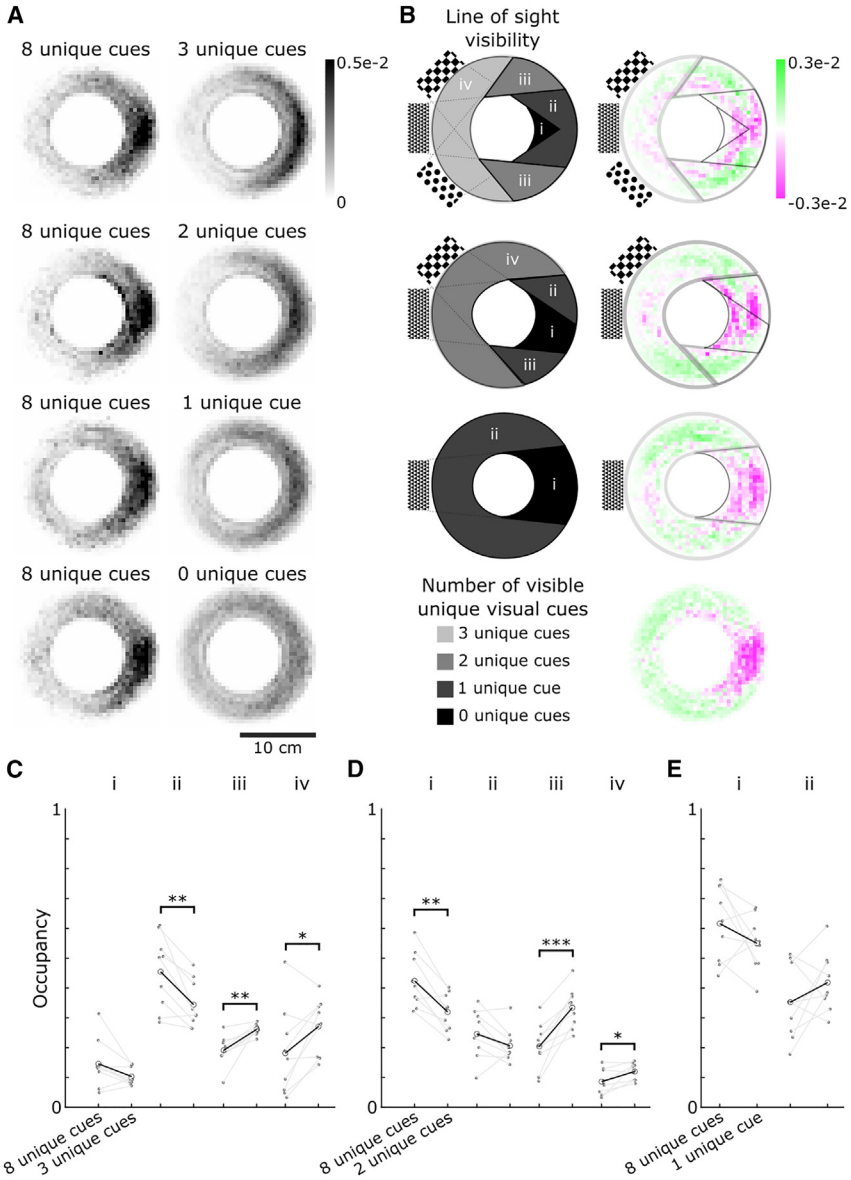

Figure 6. DC seek a line of sight to distally located unique visual cues

(A) Normalized heatmaps depicting fish positions before and after cue manipulations during the LIGHT phase. (n = 9 groups).

(B) Left: diagrams depicting discrete regions, color-coded by the number of visually accessible unique visual cues, measured by direct line of sight. Right: normalized difference heatmap reflect the change in positions after the cue manipulation during the LIGHT phase. Positive values indicate areas in which the fish spent more time following the cue manipulation.

(C–E) Pairwise comparisons of occupancy for each zone during the LIGHT phase (labeled with Roman numerals, as depicted in B). Individual solid points and thin gray lines represent individual groups. Open circles and thick black lines represent mean across groups.

Paired t test; *p < 0.05, **p < 0.01, ***p < 0.001; (C) left to right, p = 0.0066, p = 0.0025, p = 0.0393; (D) left to right, p = 0.0012, p = 5.68e−4, p = 0.016. See also Figure S6.

however, still with a bias toward remaining near the reward location (Figures 6C–6E). This suggests a strategy in which frequent visual updates of the location of the distal visual cues are required for DC to orient themselves within the annular arena.

DISCUSSION

We developed a spatial navigation task for adult DC inspired by the Morris water maze,[23] using their preference to swim in dark regions (or avoid bright regions) (Figure 1) as a motivating stimulus. We found that DC were able to anticipate the location of a future reward location (Figure 2) and that they utilized visual cues in the environment to solve the task (Figures 3A and 3B). When cues were shuffled, we found that, for some groups of fish, a single proximal cue is sufficient to be used as a landmark while, for other groups, distal cues were also used (Figure 3C). To distinguish between the relative importance of distal and proximal cues, we explored whether DC could successfully navigate with only partially occluded distal cues available (Figure 4), providing evidence for allocentric navigation (Figure 5A). One possible explanation is that DC use a memory-based strategy that allows them to remember the location of the visual cue in an allocentric fashion as they plan and execute their trajectory to the reward location, similar to observations in rodents.[52,54,55] Our analysis of swimming speed and the positioning of DC when proximal cues are removed suggests that, should such spatial memory exist, DC move in a manner such that at least one visual cue can be observed (Figures 5 and 6).

From prior work in rodents and goldfish, the ability to solve the Morris water maze under a variety of cue manipulations is associated with activity in the hippocampal formation (or the dorsal lateral pallium in teleost fish).[14,52] The extent to which this implies the existence of a cognitive map remains to be shown. It is plausible that egocentric spatial information, e.g., distance estimation via path integration and heading direction, also provides input to help DC solve this task,[39,58,59] although the observed strategy of seeking out at least one visual cue suggests that path integration alone would not be sufficient.

Our experiments were conducted with groups of fish, while many navigation studies focus on single animals. We used shoal cohesion as a measurement of group dynamics but ultimately did not detect differences in group cohesion between learner and non-learner groups. This does not address whether individuals within groups are better or worse at learning the task. Continuous video recording or skin dyes could be used to track and quantify individual performance across sessions

as well as to explore whether social dynamics impacts navigation.[60,61]

It is likely that the training schedule of the fish could be improved. With the current timeline, fish could swim to the reward location quickly but would then have to wait before the phototactic reward was presented. In other words, with our current paradigm, the behavior of the fish did not have a causal link to when the phototactic reward is delivered. This differs from the Morris water maze, in which rodents are immediately rewarded when they discover a hidden platform and are able to stand on the platform.

We found a major difference in the performance of DC in the annular and open arenas. The proximal cue removal manipulations transiently perturbed the performance of DC for a coupled cue rotation (Figure 4C), while the same manipulation did not in the open arena (Figure 3B). This perturbation might be related to the specific timing we chose for the proximal cue removal experiments, including lengthening the DARK phase to 2 min and adding a 10-min dark phase between manipulations. Although we intended these durations to allow sufficient time for DC to disperse in the annular arena, we have not measured how long the memory of the visual environment persists in darkness. The transient perturbation we observed may therefore reflect DC reacquiring the ability to solve the task in what, from their perspective, is a novel environment. Future experiments are needed to explore the persistence of the spatial memory.

In other fish species, the ability to navigate to a reward in the absence of proximal visual cues, as we observed in DC, has been interpreted as evidence for allocentric navigation.[13] Given prior work in other teleost fish,[13,14,62–65] it is plausible that spatially tuned neurons[25–27] exist in the DC brain. The central nervous system of adult DC is well within current technological capabilities of whole-brain optical imaging,[66,67] and thus an unbiased sampling of neuronal activity could be performed to not only identify putative spatially tuned neurons but also to study their role in brain-wide navigation circuits. Additionally, DC offer the exciting possibility in which both whole-brain functional imaging and synaptic-resolution connectomics can be conducted to investigate the neuronal circuitry of spatial navigation in an adult vertebrate brain, providing further insight into vertebrate learning and memory.

STAR★METHODS

Detailed methods are provided in the online version of this paper and include the following:

SUPPLEMENTAL INFORMATION

Supplemental information can be found online at https://doi.org/10.1016/j.cub.2023.11.030.

ACKNOWLEDGMENTS

We thank Benjamin Judkewitz for providing the initial stock of *Danionella cerebrum* used in this study and guidance on the husbandry of DC. Funding for this work was provided by the Max Planck Society.

AUTHOR CONTRIBUTIONS

Conceptualization, T.J.L. and K.L.B.; methodology, T.J.L. and K.L.B.; software, T.J.L.; validation, T.J.L.; formal analysis, T.J.L.; investigation, T.J.L.; writing – original draft, T.J.L.; writing – review & editing, T.J.L. and K.L.B.; funding acquisition, K.L.B.; resources, K.L.B.; visualization, T.J.L.; supervision, K.L.B.

DECLARATION OF INTERESTS

The authors declare no competing interests.

Received: June 19, 2023
Revised: October 6, 2023
Accepted: November 14, 2023
Published: December 8, 2023

REFERENCES

1. Capaldi, E.A., Robinson, G.E., and Fahrback, S.E. (1999). NEUROETHOLOGY OF SPATIAL LEARNING: the birds and the bees. Annu. Rev. Psychol. *50*, 651–682.
2. Menzel, R., Greggers, U., Smith, A., Berger, S., Brandt, R., Brunke, S., Bundrock, G., Hülse, S., Plümpe, T., Schaupp, F., et al. (2005). Honey bees navigate according to a map-like spatial memory. Proc. Natl. Acad. Sci. USA *102*, 3040–3045.
3. Ofstad, T.A., Zuker, C.S., and Reiser, M.B. (2011). Visual place learning in *Drosophila melanogaster*. Nature *474*, 204–207.
4. Healy, S.D., and Hurly, T.A. (2004). Spatial learning and memory in birds. Brain Behav. Evol. *63*, 211–220.
5. Tolman, E.C. (1948). Cognitive maps in rats and men. Psychol. Rev. *55*, 189–208.
6. Olton, D.S., and Samuelson, R.J. (1976). Remembrance of places passed: spatial memory in rats. J. Exp. Psychol.: Anim. Behav. Processes *2*, 97–116.
7. Genzel, D., Yovel, Y., and Yartsev, M.M. (2018). Neuroethology of bat navigation. Curr. Biol. *28*, R997–R1004.
8. Courellis, H.S., Nummela, S.U., Metke, M., Diehl, G.W., Bussell, R., Cauwenberghs, G., and Miller, C.T. (2019). Spatial encoding in primate hippocampus during free navigation. PLOS Biol. *17*, e3000546.
9. Nourizonoz, A., Zimmermann, R., Ho, C.L.A., Pellat, S., Ormen, Y., Prévost-Solié, C., Reymond, G., Pifferi, F., Aujard, F., Herrel, A., and Huber, D. (2020). EthoLoop: automated closed-loop neuroethology in naturalistic environments. Nat. Methods *17*, 1052–1059.
10. Epstein, R.A., Patai, E.Z., Julian, J.B., and Spiers, H.J. (2017). The cognitive map in humans: spatial navigation and beyond. Nat. Neurosci. *20*, 1504–1513.
11. Vargas, J.P., López, J.C., Salas, C., and Thinus-Blanc, C. (2004). Encoding of geometric and featural spatial information by goldfish (*Carassius auratus*). J. Comp. Psychol. *118*, 206–216.

12. Saito, K., and Watanabe, S. (2005). Experimental analysis of spatial learning in goldfish. Psychol. Rec. *55*, 647–662.
13. Durán, E., Ocaña, F.M., Broglio, C., Rodríguez, F., and Salas, C. (2010). Lateral but not medial telencephalic pallium ablation impairs the use of goldfish spatial allocentric strategies in a "hole-board" task. Behav. Brain Res. *214*, 480–487.
14. Broglio, C., Rodríguez, F., Gómez, A., Arias, J.L., and Salas, C. (2010). Selective involvement of the goldfish lateral pallium in spatial memory. Behav. Brain Res. *210*, 191–201.
15. Sison, M., and Gerlai, R. (2010). Associative learning in zebrafish (Danio rerio) in the plus maze. Behav. Brain Res. *207*, 99–104.
16. Aoki, R., Tsuboi, T., and Okamoto, H. (2015). Y-maze avoidance: an automated and rapid associative learning paradigm in zebrafish. Neurosci. Res. *91*, 69–72.
17. Lee, S.A., Ferrari, A., Vallortigara, G., and Sovrano, V.A. (2015). Boundary primacy in spatial mapping: evidence from zebrafish (*Danio rerio*). Behav. Processes *119*, 116–122.
18. Yashina, K., Tejero-Cantero, Á., Herz, A., and Baier, H. (2019). Zebrafish exploit visual cues and geometric relationships to form a spatial memory. iScience *19*, 119–134.
19. Tsang, B., Venditti, V., Javier, C.M., and Gerlai, R. (2023). The ram cichlid (*Mikrogeophagus ramirezi*) learns an associative task: a new fish species for memory research. Sci. Rep. *13*, 13781.
20. Wood, R.A., Bauza, M., Krupic, J., Burton, S., Delekate, A., Chan, D., and O'Keefe, J. (2018). The honeycomb maze provides a novel test to study hippocampal-dependent spatial navigation. Nature *554*, 102–105.
21. Rosenberg, M., Zhang, T., Perona, P., and Meister, M. (2021). Mice in a labyrinth show rapid learning, sudden insight, and efficient exploration. eLife *10*, e66175.
22. de Cothi, W., Nyberg, N., Griesbauer, E.M., Ghanamé, C., Zisch, F., Lefort, J.M., Fletcher, L., Newton, C., Renaudineau, S., Bendor, D., et al. (2022). Predictive maps in rats and humans for spatial navigation. Curr. Biol. *32*, 3676–3689.e5.
23. Morris, G.M. (1981). Spatial localization does not require the presence of local cues. Learn. Mem. *12*, 239–260.
24. Sosa, M., and Giocomo, L.M. (2021). Navigating for reward. Nat. Rev. Neurosci. *22*, 472–487.
25. O'Keefe, J., and Dostrovsky, J. (1971). The hippocampus as a spatial map. Preliminary evidence from unit activity in the freely-moving rat. Brain Res. *34*, 171–175.
26. Taube, J.S., Muller, R.U., and Ranck, J.B. (1990). Head-direction cells recorded from the postsubiculum in freely moving rats. I. Description and quantitative analysis. J. Neurosci. *10*, 420–435.
27. Fyhn, M., Molden, S., Witter, M.P., Moser, E.I., and Moser, M.B. (2004). Spatial representation in the entorhinal cortex. Science *305*, 1258–1264.
28. Solstad, T., Boccara, C.N., Kropff, E., Moser, M.B., and Moser, E.I. (2008). Representation of geometric borders in the entorhinal cortex. Science *322*, 1865–1868.
29. Nguyen, J.P., Shipley, F.B., Linder, A.N., Plummer, G.S., Liu, M., Setru, S.U., Shaevitz, J.W., and Leifer, A.M. (2016). Whole-brain calcium imaging with cellular resolution in freely behaving *Caenorhabditis elegans*. Proc. Natl. Acad. Sci. USA *113*, E1074–E1081.
30. Voleti, V., Patel, K.B., Li, W., Perez Campos, C.P., Bharadwaj, S., Yu, H., Ford, C., Casper, M.J., Yan, R.W., Liang, W., et al. (2019). Real-time volumetric microscopy of in vivo dynamics and large-scale samples with SCAPE 2.0. Nat. Methods *16*, 1054–1062.
31. Lemon, W.C., Pulver, S.R., Höckendorf, B., McDole, K., Branson, K., Freeman, J., and Keller, P.J. (2015). Whole-central nervous system functional imaging in larval Drosophila. Nat. Commun. *6*, 7924.
32. Mann, K., Gallen, C.L., and Clandinin, T.R. (2017). Whole-brain calcium imaging reveals an intrinsic functional network in drosophila. Curr. Biol. *27*, 2389–2396.e4.
33. Schaffer, E.S., Mishra, N., Whiteway, M.R., Li, W., Vancura, M.B., Freedman, J., Patel, K.B., Voleti, V., Paninski, L., Hillman, E.M.C., Abbott, L.F., and Axel, R. (2023). The spatial and temporal structure of neural activity across the fly brain. Nat. Commun. *14*, 1–15.
34. Ahrens, M.B., Li, J.M., Orger, M.B., Robson, D.N., Schier, A.F., Engert, F., and Portugues, R. (2012). Brain-wide neuronal dynamics during motor adaptation in zebrafish. Nature *485*, 471–477.
35. Kim, D.H., Kim, J., Marques, J.C., Grama, A., Hildebrand, D.G.C., Gu, W., Li, J.M., and Robson, D.N. (2017). Pan-neuronal calcium imaging with cellular resolution in freely swimming zebrafish. Nat. Methods *14*, 1107–1114.
36. White, J.G., Southgate, E., Thomson, J.N., and Brenner, S. (1986). The structure of the nervous system of the nematode *Caenorhabditis elegans*. Philos. Trans. R. Soc. Lond. B Biol. Sci. *314*, 1–340.
37. Scheffer, L.K., Xu, C.S., Januszewski, M., Lu, Z., Takemura, S.Y., Hayworth, K.J., Huang, G.B., Shinomiya, K., Maitlin-Shepard, J., Berg, S., et al. (2020). A connectome and analysis of the adult drosophila central brain. eLife *9*, 1–74.
38. Svara, F., Förster, D., Kubo, F., Januszewski, M., dal Maschio, M., Schubert, P.J., Kornfeld, J., Wanner, A.A., Laurell, E., Denk, W., and Baier, H. (2022). Automated synapse-level reconstruction of neural circuits in the larval zebrafish brain. Nat. Methods *19*, 1357–1366.
39. Petrucco, L., Lavian, H., Wu, Y.K., Svara, F., Štih, V., and Portugues, R. (2023). Neural dynamics and architecture of the heading direction circuit in zebrafish. Nat. Neurosci. *26*, 765–773.
40. Favre-Bulle, I.A., Vanwalleghem, G., Taylor, M.A., Rubinsztein-Dunlop, H., and Scott, E.K. (2018). Cellular-resolution imaging of vestibular processing across the larval zebrafish brain. Curr. Biol. *28*, 3711–3722.e3.
41. Migault, G., van der Plas, T.L., Trentesaux, H., Panier, T., Candelier, R., Proville, R., Englitz, B., Debrégeas, G., and Bormuth, V. (2018). Whole-Brain calcium imaging during physiological vestibular stimulation in larval zebrafish. Curr. Biol. *28*, 3723–3735.e6.
42. Lin, Q., Manley, J., Helmreich, M., Schlumm, F., Li, J.M., Robson, D.N., Engert, F., Schier, A., Nöbauer, T., and Vaziri, A. (2020). Cerebellar neurodynamics predict decision timing and outcome on the single-trial level. Cell *180*, 536–551.e17.
43. Markov, D.A., Petrucco, L., Kist, A.M., and Portugues, R. (2021). A cerebellar internal model calibrates a feedback controller involved in sensorimotor control. Nat. Commun. *12*, 6694.
44. Sy, S.K.H., Chan, D.C.W., Chan, R.C.H., Lyu, J., Li, Z., Wong, K.K.Y., Choi, C.H.J., Mok, V.C.T., Lai, H.M., Randlett, O., et al. (2023). An optofluidic platform for interrogating chemosensory behavior and brainwide neural representation in larval zebrafish. Nat. Commun. *14*, 227.
45. Valente, A., Huang, K.H., Portugues, R., and Engert, F. (2012). Ontogeny of classical and operant learning behaviors in zebrafish. Learn. Mem. *19*, 170–177.
46. Schulze, L., Henninger, J., Kadobianskyi, M., Chaigne, T., Faustino, A.I., Hakiy, N., Albadri, S., Schuelke, M., Maler, L., del Bene, F., and Judkewitz, B. (2018). Transparent *Danionella translucida* as a genetically tractable vertebrate brain model. Nat. Methods *15*, 977–983.
47. Penalva, A., Bedke, J., Cook, E.S.B., Barrios, J.P., Bertram, E.P.L., and Douglass, A.D. (2018). Establishment of the miniature fish species *Danionella translucida* as a genetically and optically tractable neuroscience model. Preprint at bioRxiv. https://doi.org/10.1101/444026.
48. Britz, R., Conway, K.W., and Rüber, L. (2021). The emerging vertebrate model species for neurophysiological studies is Danionella cerebrum, new species (Teleostei: Cyprinidae). Sci. Rep. *11*, 18942.
49. Akbari, N., Tatarsky, R.L., Kolkman, K.E., Fetcho, J.R., Bass, A.H., and Xu, C. (2022). Whole-brain optical access in a small adult vertebrate with two- and three-photon microscopy. iScience *25*, 105191.
50. Zada, D., Schulze, L., Yu, J.-H., Tarabishi, P., Napoli, J.L., and Lovett-Barron, M. (2023). Development of neural circuits for social motion perception in schooling fish. Preprint at bioRxiv. https://doi.org/10.1101/2023.10.25.563839.

51. Hoffmann, M., and Judkewitz, B. (2019). Diffractive oblique plane microscopy. Optica *6*, 1166–1170.
52. Zhao, X., Wang, Y., Spruston, N., and Magee, J.C. (2020). Membrane potential dynamics underlying context-dependent sensory responses in the hippocampus. Nat. Neurosci. *23*, 881–891.
53. Davidson, J.D., Sosna, M.M.G., Twomey, C.R., Sridhar, V.H., Leblanc, S.P., and Couzin, I.D. (2021). Collective detection based on visual information in animal groups. J. R. Soc. Interface *18*, 20210142.
54. Collett, T.S., and Graham, P. (2004). Animal navigation: path integration, visual landmarks and cognitive maps. Curr. Biol. *14*, R475–R477.
55. Chan, E., Baumann, O., Bellgrove, M.A., and Mattingley, J.B. (2012). From objects to landmarks: the function of visual location information in spatial navigation. Front. Psychol. *3*, 304.
56. Eichenbaum, H., Stewart, C., and Morris, R.G.M. (1990). Hippocampal representation in place learning. J. Neurosci. *10*, 3531–3542.
57. Liu, Y., Carmer, R., Zhang, G., Venkatraman, P., Brown, S.A., Pang, C.P., Zhang, M., Ma, P., and Leung, Y.F. (2015). Statistical analysis of zebrafish locomotor response. PLoS One *10*, e0139521.
58. Sibeaux, A., Karlsson, C., Newport, C., and Burt de Perera, T.B. de (2022). Distance estimation in the goldfish (Carassius auratus). Proc. Biol. Sci. *289*, 20221220.
59. Yang, E., Zwart, M.F., James, B., Rubinov, M., Wei, Z., Narayan, S., Vladimirov, N., Mensh, B.D., Fitzgerald, J.E., and Ahrens, M.B. (2022). A brainstem integrator for self-location memory and positional homeostasis in zebrafish. Cell *185*, 5011–5027.E20.
60. Pérez-Escudero, A., Vicente-Page, J., Hinz, R.C., Arganda, S., and de Polavieja, G.G. (2014). idTracker: tracking individuals in a group by automatic identification of unmarked animals. Nat. Methods *11*, 743–748.
61. Walter, T., and Couzin, I.D. (2021). Trex, a fast multi-animal tracking system with markerless identication, and 2D estimation of posture and visual fields. eLife *10*, 1–73.
62. Ocaña, F.M., Uceda, S., Arias, J.L., Salas, C., and Rodríguez, F. (2017). Dynamics of goldfish subregional hippocampal pallium activity throughout spatial memory formation. Brain Behav. Evol. *90*, 154–170.
63. Fotowat, H., Lee, C., Jun, J.J., and Maler, L. (2019). Neural activity in a hippocampus-like region of the teleost pallium is associated with active sensing and navigation. eLife *8*, e44119.
64. Vinepinsky, E., Cohen, L., Perchik, S., Ben-Shahar, O., Donchin, O., and Segev, R. (2020). Representation of edges, head direction, and swimming kinematics in the brain of freely-navigating fish. Sci. Rep. *10*, 14762.
65. Cohen, L., Vinepinsky, E., Donchin, O., and Segev, R. (2023). Boundary vector cells in the goldfish central telencephalon encode spatial information. PLoS Biol. *21*, e3001747.
66. Ahrens, M.B., Orger, M.B., Robson, D.N., Li, J.M., and Keller, P.J. (2013). Whole-brain functional imaging at cellular resolution using light-sheet microscopy. Nat. Methods *10*, 413–420.
67. Takanezawa, S., Saitou, T., and Imamura, T. (2021). Wide field light-sheet microscopy with lens-axicon controlled two-photon Bessel beam illumination. Nat. Commun. *12*, 2979.

Please cite this article in press as: Lee and Briggman, Visually guided and context-dependent spatial navigation in the translucent fish *Danionella cerebrum*, Current Biology (2023), https://doi.org/10.1016/j.cub.2023.11.030

STAR★METHODS

KEY RESOURCES TABLE

REAGENT or RESOURCE	SOURCE	IDENTIFIER
Experimental models: Organisms/strains		
Danionella cerebrum wild-type	MPINB core animal facility	N/A
Software and algorithms		
MATLAB 2019b/2020a	MathWorks	N/A
Analysis code	This paper	https://doi.org/10.17617/3.OL0FHH
Deposited data		
Analyzed data	This paper	https://doi.org/10.17617/3.OL0FHH

RESOURCE AVAILABILITY

Lead contact

Further information and requests for resources should be directed to and will be fulfilled by the lead contact, Timothy J. Lee (timothy.lee@mpinb.mpg.de).

Materials availability

This study did not generate new unique reagents.

Data and code availability

All data reported in this paper as well as all code for controlling behavioral experiments, data preprocessing, data analysis, and figure generation are available at https://doi.org/10.17617/3.OL0FHH. Raw behavioral videos can be made available upon request. Any additional information required to reanalyze the data reported in this paper will be made available from the lead contact upon request. DOI is also given in the key resources table.

EXPERIMENTAL MODEL AND SUBJECT DETAILS

For experiments with *Danionella cerebrum* (DC), wild-type, adult (age 2.5 to 5 months post fertilization (mpf)) fish, of either sex, were used. DC were maintained in group housing with stock density ~3 fish/L of water in 3.5 liter tanks (Techniplast). Water conditions were maintained at ~26.5 °C, pH 7.5, and conductivity 350 μS. Adult DC were manually fed live *Artemia*, twice per day. Silicone tubes, approximately 5 cm long and 1 cm in diameter were placed in the tanks to facilitate breeding.[46]

For experiments with *Danio rerio* (DR), wild-type (*NHGRI-1* strain), juvenile (3–4 weeks post fertilization) fish, of either sex, were used. DR were maintained in group housing with stock density ~3 fish/L of water in 3.5 liter tanks (Techniplast). Water conditions were maintained at ~28.0 °C, pH 7.5, and conductivity 400 μS. DR were manually fed live *Artemia*, twice per day.

All animal experiments were conducted in accordance with the animal welfare laws of the state of North Rhine-Westphalia in Germany and approved by the responsible governmental agency, LANUV (Ministerium für Umwelt, Landwirtschaft, Natur- und Verbraucherschutz des Landes Nordrhein-Westfalen).

METHOD DETAILS

Experimental setup

The behavioral arena, used for all experiments, was a transparent, circular, acrylic tank with 200 mm inner diameter, 10 mm wall thickness, 70 mm height, and 3 mm floor thickness. Tanks were filled to a depth of ~50 mm with fresh water with water properties suited to DC or DR, according to the species tested. White standard-weight printer paper was placed beneath the tank. A digital projector (ViewSonic, M1 LED projector), mounted 50 cm above the tank, provided illumination onto the paper from above. The projector was controlled remotely via MATLAB (MathWorks), and grayscale values ranging from 0 to 255 were used to provide environmental illumination ranging from 3 to 1530 lux, respectively. Luminance was measured with a pre-calibrated light meter (Voltcraft, MS-200 LED). Depending on the behavioral experiment, different visual cues, all printed on paper, were wrapped around the outer wall of the tank. For phototaxis experiments (Figure 1), gray paper was wrapped around the tank. For spatial navigation experiments (Figures 2,

Please cite this article in press as: Lee and Briggman, Visually guided and context-dependent spatial navigation in the translucent fish *Danionella cerebrum*, Current Biology (2023), https://doi.org/10.1016/j.cub.2023.11.030

3, and 4), eight distinct, black and white, visual cues (or a subset thereof) were used. The eight patterns used were a checkboard, vertical stripes, horizontal stripes, circles, triangles, triangles with circles, diamonds, and X's (Data S1). Each cue subtended 45 degrees of the tank's circumference. The cues were designed in Inkscape, printed on standard printer paper, cut out, wrapped manually around the tank, and taped in place. Magnetic tape was used for ease of installation and removal. Tactile references (e.g., pieces of tape) were used to maintain consistent installation of the cues in darkness. Behavioral recordings were made using a USB camera (Basler acA 2040-90uc, with lens TS1614-MP F1.4 f16mm 1″) mounted above the tank, controlled remotely via MATLAB, with infrared illumination (Raytec, RM25-30; 850 nm) installed below the tank and a long-pass filter (Thorlabs, FGL780S) installed in front of the camera to filter out visible light. All experiments were recorded at 25 fps, with resolution of ~1400 x 1400 pixels. A ceramic terrarium heater (Elstein, IOT75) was placed near the tank to maintain the water temperature at ~26.5 °C. A custom shutter was installed in front of the projector and controlled via an Arduino (Uno Rev. 3) to remotely shutter the background illumination of the projector in the experimental setup during dark phases and cue manipulations. Fish were allowed to habituate in the arena for at least 24 hours prior to all experiments. Fish were maintained on 10-hour/14-hour light/dark cycle. During the light cycle on the habituation day, the projector backlight illumination was used to provide illumination to the tank, resulting in dim illumination at 3 lux. During the night cycle, all light was shuttered via the remotely controlled shutter such that the experiment setup was completely dark (0 lux). The setup in its entirety was enclosed in a custom black-out box and installed on vibration-dampening sorbothane pads to reduce external environmental disturbances. Prior to experiments on each day, fish were manually fed Artemia and allowed to eat for 30 to 60 minutes. Afterwards, the water in the tank was manually flushed to remove detritus and refilled with fresh water. Experiments were started roughly 60 minutes after cleaning and feeding to allow any stress induced by the tank disturbance to dissipate.

Due to the inability to automatically change the location of the visual cues on a trial-by-trial basis in our current paradigm, it was not possible for us to control the starting location of the fish. This would be desirable in order to potentially reduce the trial-to-trial variability in swimming trajectories. The experimental design could be improved upon by using digital displays to create environmental visual cues, which could then be changed or moved on a trial-by-trial basis. We opted for physical paper cues based on initial experiments that indicated a sensitivity to the illumination of projected cues but did not further explore digital projection.

DC exhibit negative phototaxis

Phototaxis was tested in individual adult DC (n = 10), groups of three DC (n = 10 groups of three fish; 30 total fish), and groups of three juvenile ZF (n = 10 groups of three fish; 30 total fish) (Figures 1 and S1). The tank brightness was set using grayscale values = {0, 16, 32, 64, 128, 196, 255} resulting in a series of seven luminance values = {3, 5, 13, 50, 305, 962, 1530 lux}, respectively. We took care to ensure the tank was uniformly illuminated by the projector to avoid any unintentional luminance gradients. Each luminance value was tested by illuminating half of the tank with the specified luminance, while the other half was kept at 3 lux (the backlight intensity of the LED projector). Each luminance value was tested four times such that the illuminated half of the tank was rotated either 0, 90, 180, or 270 degrees to control for any innate place preferences. Accordingly, each experiment was composed of 28 trials (seven luminance values times four orientations of the stimulus). For 7 out of the 10 groups of three DC, each trial lasted five minutes with a five minute inter-trial interval, during which the projector was shuttered (0 lux). For all remaining groups of adult DC, for the single DC, and for the groups of juvenile ZF experiments, each trial lasted ten minutes with a ten minute inter-trial interval, during which the projector was shuttered (0 lux). The luminance and orientation of the stimulus were presented in a pseudorandom fashion.

DC are capable of learning a Morris water maze-like spatial navigation task

Spatial navigation in the open-tank, Morris Water Maze-like task was tested on groups of three adult DC (n = 77 groups of three fish) (Figures 2, 3, and S2). The fish were habituated in the open behavioral arena for at least 24 hours with the set of 8 distinct visual cues installed, as described above. Fish were trained using a fixed trial duration experiment structure, in which each trial was composed of four phases and presented in the following order: (1) DIM, whole-tank, low-luminance (3 lux) illumination, duration 60 seconds; (2) LIGHT, whole tank, high-luminance (1530 lux) illumination, duration 20 seconds; (3) REWARD, whole tank, high-luminance (1530 lux) illumination with a localized region (8 cm diameter circle, offset 5 cm from the tank center) of low-luminance (3 lux), duration 45 seconds; (4) DARK, all light shuttered (0 lux), duration 60 seconds. To mitigate stress in response to sudden changes in luminance, the transition in luminance from DIM to LIGHT was presented along a linear ramp across 5 seconds; these five seconds preceded the LIGHT phase and were excluded from analysis. Each experiment consisted of 80 trials. For all 77 groups of fish, the first 30 trials were identical. After each experiment, the performance (see section quantification and statistical analysis) of the fish was analyzed. If the performance of the fish did not asymptotically approach 4 cm within the first 30 trials, the experiment was repeated on the following day, for a maximum of five consecutive days of training, after which the fish were deemed 'non-learners'. On average, the fish learned to solve the spatial navigation task within 3 ± 1 days (mean ± standard deviation). 24 groups of fish were classified as non-learners (24 / 77); 53 groups of fish were classified as learners (53 / 77). For learners, the data shown is only from the last day of training. For non-learners, data is from the fifth day of training. In our earliest experiments ('Cue removal' and 'Sham cue removal') the specific visual cue located in front of the reward location was randomized, and we observed that the fish were able to learn to solve the task under a variety of cue configurations. For our later experiments ('Coupled cue rotation', 'Uncoupled cue rotation', and 'Cue shuffle'), we kept the cue configuration constant, with the horizontal stripes directly in front of the reward location. Additionally, between different groups of fish, the orientation of the set of visual cues was rotated either 0, 90, 180, or 270 degrees to control for possible innate place preferences within the tank.

Please cite this article in press as: Lee and Briggman, Visually guided and context-dependent spatial navigation in the translucent fish *Danionella cerebrum*, Current Biology (2023), https://doi.org/10.1016/j.cub.2023.11.030

DC perform visually guided spatial navigation

53 groups of three fish (159 total fish) were used to investigate visually-guided spatial navigation in DC divided amongst the following cue manipulation experiments: Cue removal (n = 10 groups of fish), sham cue manipulations (n = 10 groups of fish), uncoupled cue rotation (n = 10 groups of fish), coupled cue rotation (n = 14 groups of fish), and cue shuffle (n = 9 groups of fish) (Figures 3, S3, and S4). As discussed in the previous section, these 53 groups were the groups of fish classified as learners. Experiments used the same fixed trial duration experiment structure described above with the same experiment phases. Experiments consisted of 80 consecutive trials with cue manipulations occurring after trial 30 and after trial 50. The experiments were run in an automated fashion using custom software written in MATLAB to acquire the behavioral recordings, control the experiment timing structure, control the digital projector, and control the projector shutter. For experiments requiring manual cue manipulations, a pause was inserted in the code to allow for manual cue manipulation. Any cue manipulations that were performed manually were performed in darkness in the experimental setup and experimental room such that the fish were unable to see the changing of the cues. Tactile references were placed around the tank to guide cue changes in the dark.

The first cue manipulation was performed after trial 30. The different cue manipulations were as follows: For cue removal experiments, the set of 8 visual cues was manually replaced with gray paper; for sham cue manipulation experiments, the set of 8 visual cues were removed and then reinstalled; for uncoupled cue rotation experiments, the cues were left in place, but the reward location was rotated relative to the cues by 90, 180, or 270 degrees using the digital projector; for coupled cue rotation experiments, the cues were manually rotated by 90, 180, or 270 degrees and the reward location rotated by the same degree, and for the cue shuffle experiments, the set of 8 distinct visual cues was replaced with a shuffled iteration of the same visual cues, such that all the visual cues except for the cue directly in front of the reward location were moved to a new location. A second cue manipulation was performed after trial 50: For the cue removal experiments, the initial set of 8 visual cues was restored; for the sham cue manipulation experiments, an additional sham cue manipulation was conducted; for the uncoupled cue rotation experiment, the initial alignment between cues and reward location was restored; for the coupled cue rotation experiments, the cues and reward location were rotated back to their initial positions; for the cue shuffle experiments, the initial, unshuffled set of 8 visual cues was restored.

Context-dependent spatial navigation in DC

To test context-dependent spatial navigation in DC, we tested 10 groups of three fish (30 total fish) (Figures 4, 5, 6, S5, and S6). For these experiments, a visual blockade (black Delrin, 50 mm height, 100 mm diameter, 2 mm thickness) was placed in the center of the tank. The blockade was made with a sloping outer wall to match the angle of view of the camera. The fish were habituated to the tank with the blockade installed. The radius of the circular reward zone was increased to 5 cm to adjust for portions of the reward zone occluded by the blockade. These experiments were conducted using the same fixed trial duration experiment structure as previously outlined with the same experiment phases, but with the timing slightly changed: (1) DIM, whole-tank, low-luminance (3 lux) illumination, duration 30 seconds; (2) LIGHT, whole tank, high-luminance (1530 lux) illumination, duration 20 seconds; (3) REWARD, whole tank, high-luminance (1530 lux) illumination with a localized region (10 cm diameter circle, offset 5 cm from the tank center) of low-luminance (3 lux), duration 45 seconds; (4) DARK, all light shuttered (0 lux), duration 120 seconds. To mitigate stress in response to sudden changes in luminance, the transition in luminance from DIM to LIGHT was presented along a linear ramp across 5 seconds; these five seconds preceded the LIGHT phase and were excluded from analysis. The fish were trained with 8 unique visual cues for 90 consecutive trials, with either a ±120° coupled cue rotation conducted after trial 45, followed by a ten minute pause during which the fish were kept in complete darkness. After each day of training, the distance-to-target (i.e., 'performance') during the LIGHT phase across all trials was analyzed. If the performance of the fish did not asymptotically approach 5 cm, the experiment was repeated on the following day, for a maximum of five consecutive days of training, after which the fish were deemed 'non-learners'. 1 group was classified as 'non-learner' (1 / 10). For 'learners', the fish learned to solve the spatial navigation task within 3 ± 1 days (mean ± standard deviation). Following the last training day, we began the cue manipulation experiments (i.e., test days). On each test day, all cues remained on the tank, identical to that of the training days, during trials 1 to 30. Following trial 30, one of four cue manipulations was performed: five proximal (i.e., the cues closest to the reward location) cues were replaced with repeating vertical stripes (i.e., 3 unique distal cues remaining), six proximal cues were replaced with repeating vertical stripes (i.e., 2 unique distal cues remaining), seven proximal cues were replaced with repeating vertical stripes (i.e., 1 unique distal cue remaining), or all the unique cues were replaced with repeating vertical stripes. These four cue manipulations were conducted on four consecutive days in a randomized order. For the '2 unique distal cue remaining' cue manipulation, the single cue diametrically aligned with the reward and the cue immediately to its right were kept. Also, the vertical stripes were of a finer spatial frequency than that of the vertical stripes used as a unique visual cue (Data S1). From trials 31 to 50, the fish were tested under this cue manipulation. After trial 50, with the same subset of visual cues, we performed either a ±120° coupled cue rotation, and the fish were tested for 20 trials. After trial 70, the cues and the reward location were rotated back to their initial orientation and tested for 20 trials. In total, each test day was composed of 90 trials. Between each cue manipulation, we inserted a 10 minute pause, during which all light was shuttered. The initial set of 8 visual cues were restored after each experiment between test days.

QUANTIFICATION AND STATISTICAL ANALYSIS

All data and statistical analysis was conducted in MATLAB (MathWorks). To quantify all behavioral experiments, raw behavioral videos were analyzed using a custom MATLAB script. To extract the fish centroids, an image processing algorithm composed of

Please cite this article in press as: Lee and Briggman, Visually guided and context-dependent spatial navigation in the translucent fish *Danionella cerebrum*, Current Biology (2023), https://doi.org/10.1016/j.cub.2023.11.030

the following steps was used: (1) background subtraction, (2) image binarization, (3) image erosion and dilation, (4) connected-component object detection, and (5) centroid detection. Nearest neighbor sorting was used to obtain individual fish trajectories.

For phototaxis experiments, the centroid position of each fish was compared to the midline that split the tank between the dark and light portions of the tank (Figures 1C and S1B–S1D). For each video, the number of frames that each fish resided in the dark half of the tank was divided by the total number of frames to obtain the fraction of time spent in the dark half of the tank. This was then averaged across trial repeats. For phototaxis experiments, we analyzed only the first minute of each video given that, in our spatial navigation experiments, we were interested in the phototactic behavior of DC on time-scales of ~1 minute.

For the visually-guided spatial navigation experiments, once the centroids were obtained, the distance-to-target was computed for each fish for each frame of each behavioral recording (Figures 2C, 2D, 3A–3C, S2, S3B–S3D, and S4). This was obtained by taking the Euclidean distance between each fish and the center of the reward area (i.e., "target"). For brevity, the distance-to-target is referred to interchangeably as the "performance." Given the different durations of the experiment phases, we used a time-matched metric to compare across the different experiment phases. Specifically, all the distances-to-target for the last 20 seconds of the DIM phase, the entire 20 seconds of the LIGHT phase, the first 20 seconds of the REWARD phase, and the last 20 seconds of the DARK phase were taken. The distances-to-target were averaged across time for each trial. In plots depicting the distance-to-target across trials, the median (taken across different groups of fish) line is shown with shaded interquartile range. Since the geometry of the tank and the location of the target was well-defined, we were able to compute the average distance to the target drawn from a random uniform distribution of positions within the tank's area (i.e., we randomly sampled many points within the tank, computed the distance to the target for each of these points, and measured the average). We calculated this theoretical value to be 6.3 cm in the open arena and 10.2 cm for the annular arena. For plots depicting the performance across trials in the open arena, this theoretical value is shown as a horizontal dashed line and is referred to in the main text as the "chance level." Additionally, a dashed line at 4 (or 5, for the annular arena) cm is also shown, representing the radius of the reward area. For binned-trial comparisons, we binned the performance across trials 11-30 (i.e., before the cue manipulations), trials 31-50 (during the cue manipulation), and trials 61-80 (after the cue manipulations) (Figures 3D and 3E). To analyze each group's shoal cohesion during the LIGHT phase, we calculated the sum inter-fish distance across trials 1-30. To obtain the sum inter-fish distance, for each trial we calculated the sum-distance between the three fish and took the average across the entire LIGHT phase (Figures S2B and S2C).

For the proximal cue removal experiments, the distance-to-target was computed as described above (Figures 4C, 4D, and S5A). Given the different durations of the experiment phases, we used a time-matched metric to compare across the different experiment phases. Specifically, all the distances-to-target for the last 20 seconds of the DIM phase, the entire 20 seconds of the LIGHT phase, the first 20 seconds of the REWARD phase, and the last 20 seconds of the DARK phase were taken. The average velocity and sum inter-fish distance (i.e., shoal cohesion) were also analyzed according to the same time bins (Figures 5, S5B, and S5C): To obtain the average velocity for each group of fish, for each trial we pooled the instantaneous velocities of the three fish from each group and took the average across the 20-second time bin. To obtain the sum inter-fish distance, for each trial we calculated the sum-distance between the three fish and took the average across the 20-second time bin. For binned-trial comparisons, we compared the asymptotic performance of the fish during each cue manipulation; therefore, we analyzed the last ten trials of each cue manipulation trial block (Figures 4E, 5A, and 5B). Specifically, we compared the binned the performance across trials 21-30 (i.e., '8 unique cues'), trials 41-50 (i.e., 'Proximal cue removal'), trials 61-70 (i.e., 'Coupled cue rotation'), and trials 81-90 (i.e., 'Coupled cue counter-rotation'). We also used these same trial bins for generating the position heat maps (Figures 6 and S6).

Position heat maps shown in Figure 6 were generated by binning all centroids across all groups and across the corresponding trial bins into 0.5 cm x 0.5 cm spatial bins and dividing the spatial bin counts by the total number of centroids. Heat maps shown in Figures S1, S3, and S6 were generated using the same spatial binning but for individual groups. Line-of-sight zones as depicted in Figure 6B were calculated based on the minimum number of visually accessible unique cues via direct line sight at each point in the annular arena. To calculate each zone occupancy (Figures 6C–6E), for each group, centroids from trials 41-50, 61-70, and 81-90 during the LIGHT phase for each proximal cue removal experiment were binned into 0.5 cm x 0.5 cm spatial bins and then the bins counts of spatial bin were divided by the total number of centroids and summed across each zone. Thus, the total occupancy across all zones for any given group is unity and each zone occupancy remains bounded between 0 and 1.

For all statistical comparisons, we first tested each distribution for normality using the one-sample Kolmogorov-Smirnov test. For all distributions, we failed to reject the null hypothesis. For a single pair-wise comparison, we used a paired t-test (Figures 1C, 2E, and 6C–6E). For multiple distribution comparisons, we first tested for significance using a one-way analysis of variance (ANOVA) test. If any significant difference was detected, we then used a paired-sample t-test to test all pair-wise combinations for significance with *post hoc* Bonferroni correction (Figures 3D, 3E, 4E, 5A, and 5B). Statistical tests shown in Figures 3D and 3E compare performance across cue manipulations (i.e., before the cue manipulation, during the cue manipulation, and after the cue manipulation) but within groups for any given experiment (i.e., 'Cue removal', 'Sham cue removal', etc.). Statistical tests shown in Figure 4E compare performance across the cue manipulation trial bins (i.e., '8 unique cues', 'Proximal cue removal', 'Coupled cue rotation', and 'Coupled counter cue rotation') but within the groups of fish and not across experiment days. For comparing shoal cohesion versus performance for learner and non-learner groups, an F-test was performed to see if a linear regression fit significantly better than a constant-term model (Figure S2C). For comparing shoal cohesion across trials and across learner/non-learning status, we performed a repeated measures ANOVA (Figure S2C).